International Journal for Parasitology: Drugs and Drug Resistance 4 (2014) 28–36

Contents lists available at ScienceDirect

International Journal for Parasitology: Drugs and Drug Resistance

journal homepage: www.elsevier.com/locate/ijpddr

Novel *S*-adenosyl-L-methionine decarboxylase inhibitors as potent antiproliferative agents against intraerythrocytic *Plasmodium falciparum* parasites

Dina le Roux [a], Pieter B. Burger [a], Jandeli Niemand [a], Anne Grobler [b], Patricia Urbán [c,d,e], Xavier Fernàndez-Busquets [c,d,e], Robert H. Barker [f], Adelfa E. Serrano [g], Abraham I. Louw [a], Lyn-Marie Birkholtz [a,*]

[a] Department of Biochemistry, Centre for Sustainable Malaria Control, University of Pretoria, Private Bag X20, Hatfield 0028, South Africa
[b] DST/NWU Preclinical Drug Development Platform, North-West University, Potchefstroom 2531, South Africa
[c] Nanobioengineering Group, Institute for Bioengineering of Catalonia, Baldiri Reixac 10-12, Barcelona E08028, Spain
[d] Barcelona Centre for International Health Research (CRESIB), Hospital Clínic-Universitat de Barcelona, Rosselló 149-153, Barcelona E08036, Spain
[e] Biomolecular Interactions Team, Nanoscience and Nanotechnology Institute (IN2UB), University of Barcelona, Martí i Franquès 1, Barcelona E08028, Spain
[f] Genzyme Corporation, 153 Second Avenue, Waltham, MA 02451, USA
[g] University of Puerto Rico-School of Medicine, Department of Microbiology and Medical Zoology, P.O. Box 365067, San Juan PR 00936-5067, Puerto Rico

ARTICLE INFO

Article history:
Received 20 September 2013
Received in revised form 19 November 2013
Accepted 20 November 2013
Available online 5 December 2013

Keywords:
Plasmodium
Polyamines
S-adenosyl-L-methionine decarboxylase
Immunoliposomes

ABSTRACT

S-adenosyl-L-methionine decarboxylase (AdoMetDC) in the polyamine biosynthesis pathway has been identified as a suitable drug target in *Plasmodium falciparum* parasites, which causes the most lethal form of malaria. Derivatives of an irreversible inhibitor of this enzyme, 5′-{[(Z)-4-amino-2-butenyl]methylamino}-5′-deoxyadenosine (MDL73811), have been developed with improved pharmacokinetic profiles and activity against related parasites, *Trypanosoma brucei*. Here, these derivatives were assayed for inhibition of AdoMetDC from *P. falciparum* parasites and the methylated derivative, 8-methyl-5′-{[(Z)-4-aminobut-2-enyl]methylamino}-5′-deoxyadenosine (Genz-644131) was shown to be the most active. The *in vitro* efficacy of Genz-644131 was markedly increased by nanoencapsulation in immunoliposomes, which specifically targeted intraerythrocytic *P. falciparum* parasites.

© 2013 The Authors. Published by Elsevier Ltd. Open access under CC BY-NC-ND license.

1. Introduction

Polyamines (putrescine, spermidine and spermine) are critical components of cell growth and division, particularly in rapidly proliferating cells that include cancerous cells and numerous parasites (Casero and Marton, 2007; Heby et al., 2007). A number of enzymes in the biosynthesis of polyamines have been validated as suitable drug targets including ornithine decarboxylase (ODC) (Pegg, 2006) and *S*-adenosyl-L-methionine decarboxylase (AdoMetDC) (Pegg, 2009) as the two major enzymatic activities. Protozoan infections resulting in human parasitic diseases such as African sleeping sickness (caused by subspecies of *Trypanosoma brucei*), Chagas disease (*Trypanosoma cruzi*), leishmaniasis (*Leishmania* spp) and malaria (*Plasmodium* spp) are highly reliant on substantial amounts of polyamines for development and proliferation (Heby et al., 2003; Birkholtz et al., 2011). Of these diseases, malaria has a high disease incidence in most tropical regions of the world, with *Plasmodium falciparum* parasites being the most lethal.

AdoMetDC catalyses a chokepoint reaction to produce decarboxylated *S*-adenosyl-L-methionine (dcAdoMet) that is exclusively used for polyamine biosynthesis. The irreversible AdoMetDC inhibitor, 5′-{[(Z)-4-amino-2-butenyl]methylamino}-5′-deoxyadenosine (MDL73811), is 100-fold more effective than the ODC inhibitor, DL-α-difluoromethylornithine (DFMO), in curing murine *T. b. brucei* and *T. b. rhodesiense* infections. Treatment of *T. brucei* parasites

Abbreviations: AdoMet, *S*-adenosyl-L-methionine; AdoMetDC, *S*-adenosyl-L-methionine decarboxylase; dcAdoMet, decarboxylated *S*-adenosyl-L-methionine; DFMO, DL-α-difluoromethylornithine; Genz-644043, 2′-fluoro-5′-{[(Z)-4-amino-2-butenyl]methylamino}-5′-deoxyadenosine; Genz-644053, 2-chloro-5′-{[(Z)-4-amino-2-butenyl]methylamino}-5′-deoxyadenosine; Genz-644131, 8-methyl-5′-{[(Z)-4-aminobut-2-enyl]methylamino}-5′-deoxyadenosine; MDL73811, 5′-{[(Z)-4-amino-2-butenyl]methylamino}-5′-deoxyadenosine; ODC, ornithine decarboxylase.

* Corresponding author. Address: Department of Biochemistry, Centre for Sustainable Malaria Control, University of Pretoria, Room 7-14, Private Bag X20, Hatfield 0028, South Africa. Tel.: +27 12 420 2479; fax: +27 12 362 5302.
E-mail address: lbirkholtz@up.ac.za (L.-M. Birkholtz).

2211-3207 © 2013 The Authors. Published by Elsevier Ltd. Open access under CC BY-NC-ND license.
http://dx.doi.org/10.1016/j.ijpddr.2013.11.003

with MDL73811 causes an intracellular hypermethylated state due to accumulation of *S*-adenosyl-L-methionine (Byers et al., 1991) in addition to the detrimental depletion of trypanothione (the principal polyamine-dependent thiol in trypanosomes) (Yarlett et al., 1991; Willert and Phillips, 2008). AdoMetDC is considered an attractive drug target in *P. falciparum* parasites due to its unique association with ODC in a heterotetrameric bifunctional protein complex, *Pf*AdoMetDC/ODC (van Brummelen et al., 2008; Birkholtz et al., 2011; Williams et al., 2011). MDL73811 inhibits *in vitro* intraerythrocytic *P. falciparum* parasite proliferation (Wright et al., 1991; Das Gupta et al., 2005), however, this does not result in a hypermethylated state but only depletes intracellular polyamine levels, leading to cellular cytostasis (Wallace et al., 2003; van Brummelen et al., 2008; Birkholtz et al., 2011).

MDL73811, however, is not clinically useful against parasitic infectious due to poor blood brain barrier penetration, a short plasma half-life, poor oral bioavailability and limited metabolic activity (Wright et al., 1991; Das Gupta et al., 2005; Barker et al., 2009). Structure-guided design of MDL73811 derivatives, modified on the ribose and purine moieties through addition of halogens and methyl groups, resulted in a series of compounds with improved ADME toxicity profiles. These included improved aqueous solubility, decreased rates of hepatocyte and microsome clearance, minimal CYP inhibition and half the plasma protein binding capacity compared to MDL73811 (Bacchi et al., 2009; Barker et al., 2009; Hirth et al., 2009). Methylation of position 8 of the adenine group resulting in 8-methyl-5′-{[(Z)-4-aminobut-2-enyl]methylamino}-5′-deoxyadenosine (Genz-644131) displayed an increased inhibitory potency against heterologous *Tb*AdoMetDC. This compound showed improved cellular toxicity against different *T. brucei* parasite strains, with a longer plasma half-life and improved blood brain barrier penetration in *in vivo* mice (Bacchi et al., 2009; Barker et al., 2009). Here, the MDL73811 derivatives were assessed for inhibitory activity against heterologous *Pf*AdoMetDC as well as for inhibition of intraerythrocytic *P. falciparum* parasite proliferation *in vitro*.

2. Methods and materials

2.1. MDL73811 and derivatives

MDL73811 (5′-{[(Z)-4-amino-2-butenyl]methylamino}-5′-deoxyadenosine), Genz-644131 (8-methyl-5′-{[(Z)-4-amino-2-butenyl]methylamino}-5′-deoxyadenosine), Genz-644043 (2′-fluoro-5′-{[(Z)-4-amino-2-butenyl]methylamino}-5′-deoxyadenosine), and Genz-644053 (2-chloro-5′-{[(Z)-4-amino-2-butenyl]methylamino}-5′-deoxyadenosine) (Table 1) were synthesised by the Genzyme Corporation (www.genzyme.com, 2013; Hirth et al., 2009).

2.2. Recombinant PfAdoMetDC enzyme inhibition assays

The monofunctional form of *Pf*AdoMetDC (harmonised gene construct) as well as bifunctional *Pf*AdoMetDC/ODC were heterologously expressed in *Escherichia coli* BL21 Star™ (DE3) cells and purified via Strep-tag affinity chromatography as previously described (Birkholtz et al., 2004; Williams et al., 2011). To determine the enzyme inhibition activity of the MDL73811 derivatives, an isotope-based bioassay that measures the release of radiolabeled CO_2 (Birkholtz et al., 2004; Williams et al., 2011) was performed with 5 μg of either monofunctional *Pf*AdoMetDC or bifunctional *Pf*AdoMetDC/ODC in the presence of 1 μM of each derivative. Results were normalised to the specific activity (nmol/min/mg) of an uninhibited control to determine % inhibition.

2.3. Determination of the inhibition constant of Genz-644131 against PfAdoMetDC

The apparent inhibition constant ($K_i$app) of Genz-644131 was determined with Kitz and Wilson time dependent enzyme kinetics for irreversible inhibitors as described (Kitz and Wilson, 1962). Using the isotope-based bioassay described above, residual enzyme activity was measured following pre-incubation (37 °C) at fixed time intervals (2, 4 and 6 min) with varying inhibitor concentrations (0.02, 0.05 and 0.1 μM) and 1 μg of either monofunctional *Pf*AdoMetDC or bifunctional *Pf*AdoMetDC/ODC, each in duplicate. The reciprocal of the slope in the primary graph (k_{app}) was plotted against the reciprocal of the inhibitor concentrations to yield the secondary plot, from which the k_{inact} and the $K_i$app values were derived.

2.4. Homology modelling and conformational analysis

P. falciparum and *T. brucei* homology models were generated using the human AdoMetDC crystal structure (PDBid 3DZ2) as template similar to a previously described model (Wells et al., 2006). Molecular shape-based alignment between MDL73811 derivatives and the homology model was performed with vROCS (v3.1.0 OpenEyeScientific Software, Inc., Santa Fe, NM, USA, www.eyesopen.com, 2010) (Supplemental data; Fig. S1 and Table S1). Conformational analysis was performed using Conformation Search and the Minimisation module of Discovery Studio 3.0 suite (Accelrys, Inc.). Detailed methods for homology modelling, molecular shape based alignment and conformational analysis are provided in Supplemental data, S1.

2.5. In vitro cultivation of intraerythrocytic P. falciparum parasites and IC_{50} determination of MDL73811 derivatives

Intraerythrocytic *P. falciparum* parasites (strain 3D7; chloroquine sensitive) were maintained in *P. falciparum* culture media as described (Verlinden et al., 2011). Intraerythrocytic parasites were synchronised to a 95% ring stage population with a 5% sorbitol solution. The effect of MDL73811 derivatives on the proliferation of intraerythrocytic *P. falciparum* parasites at 37 °C for 96 h was determined using a SYBR Green I-based fluorescence assay as described (Verlinden et al., 2011). MDL73811 and Genz-644131 were dissolved in 1xPBS and Genz-644043 and Genz-644053 in DMSO and incubated with ring stage intraerythrocytic *P. falciparum* parasites (1% parasitaemia, 1% haematocrit) at specific concentrations, serially diluted 2-fold in culture medium (final 0.1% (v/v)) non-lethal DMSO concentration (Grobusch et al., 1998). Sigmoidal dose–response curves were fitted to the data using SigmaPlot 11.0 with non-linear regression yielding the IC_{50} values (concentration at which 50% inhibition of parasite proliferation was observed).

2.6. Determining parasite recovery following Genz-644131 inhibition

The ability of the products of polyamine metabolism to rescue parasites from the inhibitory effect of Genz-644131 was determined. Ring stage intraerythrocytic *P. falciparum* parasites (1% parasitaemia, 1% haematocrit) were treated with Genz-644131 ($2xIC_{50}$) in the presence of exogenous spermidine trichloride (non-toxic concentration, 250 μM, results not shown) and 500 μM of the polyamine oxidase inhibitor, aminoguanidine (Niemand et al., 2013), for 96 h at 37 °C and parasite proliferation determined with a SYBR Green I-based assay (Stjernborg and Persson, 1993; Lee and Sayre, 1998).

Subsequently, to determine the ability of ring stage intraerythrocytic *P. falciparum* parasites (1% parasitaemia, 1% haematocrit) to recover after Genz-644131 treatment, the latter was withdrawn

Table 1
Conformational search analysis of MDL73811 and its derivatives.

		Lowest overall energy conformation[#]	Lowest *syn* energy conformation[#]	Number of conformations generated[#]	Bioactive *syn* conformational number[*], [#]
MDL73811 5′-{[(Z)-4-amino-2-butenyl]methylamino}-5′-deoxyadenosine	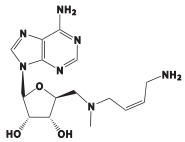	−131.6	−124.0	200	22
Genz-6441318-methyl-5′-{[(Z)-4-amino-2-butenyl]methylamino}-5′-deoxyadenosine	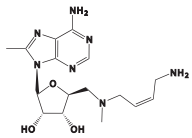	−132.9	−130.7	207	7
Genz-6440432′-fluoro-5′-{[(Z)-4-amino-2-butenyl]methylamino}-5′-deoxyadenosine	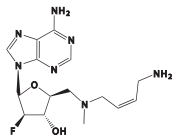	−131.0	−117.8	193	106
Genz-6440532-chloro-5′-{[(Z)-4-amino-2-butenyl]methylamino}-5′-deoxyadenosine	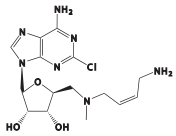	−136.0	−127.8	209	64

[#] All energies are given in kcal/mol.
[*] Generated conformations were ranked from the lowest to highest energy i.e. the bioactive *syn* conformation of Genz-644131 was ranked the 7th lowest energy conformation from 207 conformations generated.

following 24 h incubation at 37 °C at 2 × IC_{50}, the parasites washed and subsequently resuspended in normal culture media. Samples were removed at 12 h intervals over 96 h and DNA content was determined for the treated, untreated and the Genz-644131 withdrawn parasite populations using a SYBR Green I-based assay.

2.7. Spermidine uptake in intraerythrocytic P. falciparum parasites

Intraerythrocytic *P. falciparum* parasites were purified to ⩾ 95% parasitaemia with magnetic separation (Trang et al., 2004; Teng et al., 2009). [^{3}H]spermidine uptake was initiated by combining equal volumes of cell suspension and radiolabelled solution (1 μCi/ml [^{3}H]spermidine at 5 nm extracellular concentration, PerkinElmer, in 125 mM NaCl, 5 mM KCl, 20 mM glucose, 25 mM HEPES and 1 mM $MgCl_2$, pH 7.1). At predetermined time intervals following incubation at 37 °C, the reactions were terminated by dibutyl phthalate sedimentation. A 10 μl sample of the aqueous phase was transferred to a scintillation vial to determine the extracellular concentration of [^{3}H]spermidine. The remaining cell pellet was lysed with 0.1% (v/v) Triton X-100, the proteins precipitated with 5% w/v trichloroacetic acid and cell debris (including membrane fractions) removed with centrifugation before measuring the radioactivity present in the aqueous supernatant. The rapid initial association of radiolabel with the cells, due to polyamines trapped in the extracellular space as well as adhering to the cell surface was determined and subtracted from the total measured radioactivity (cmp's) to determine the intracellular concentration of polyamines. The data are given as a distribution ratio of intracellular to extracellular spermidine (Saliba et al., 1998).

2.8. Comparative IC_{50} determination of Genz-644131 incorporated with Pheriod® technology

A micellular formulation of a nanoparticle structure, Pheroid®, consisting mainly of 43.8% plant and essential ethylated and PEGylated polyunsaturated fatty acids, was prepared in incomplete RPMI 1640 medium as described (Grobler et al., 2008; Steyn et al., 2011). The suspension was subsequently filtered (0.22 μm), diluted 50 × with sterile water and homogenised with Genz-644131 powder to yield an encapsulated suspension with a final compound concentration of 23.75 mM. The encapsulation efficiency of Pheroid® was analysed with confocal laser scanning microscopy (Grobler et al., 2007). Subsequently, ring stage intraerythrocytic *P. falciparum* parasites (1% parasitaemia, 1% haematocrit) were treated with Genz-644131 encapsulated Pheroid® at a 20-fold dilution (24 μM initial starting concentration) and incubated for 96 h at 37 °C. Parasite proliferation of cell suspensions treated with Genz-644131 encapsulated into Pheroid® was determined, and normalised against non Genz-644131 encapsulating Pheroid® in order to derive the IC_{50} value using a SYBR Green I-based assay.

2.9. Comparative IC_{50} determination of Genz-644131 with immunoliposomes

Immunoliposomes were prepared by the lipid film hydration method (MacDonald et al., 1991) and covalently functionalised with IgG antibody fragments prepared specifically for intraerythrocytic *P. falciparum* parasites (Urbán et al., 2011a). For encapsulation of Genz-644131, 1.74 mg of the compound was incorporated into a 1.5 ml immunoliposome suspension to give a final concentration of encapsulated Genz-6644131 at 30 μM (10% encapsulation efficiency). Ring stage intraerythrocytic *P. falciparum* parasites (1% parasitaemia, 1% haematocrit) were treated with Genz-644131 encapsulated immunoliposomes at a 50-fold dilution (0.6 μM starting concentration) and incubated for 96 h at 37 °C. Parasite proliferation of cell suspensions treated with Genz-644131 encapsulated into immunoliposomes was determined as described above.

2.10. Statistical analyses

All data are representative of at least three independent biological experiments (n ⩾ 3), each performed in triplicate. Statistical analysis was performed using either paired or unpaired Student's

t-tests. Data were analysed using GraphPad Prism 5.0 or SigmaPlot 11.0.

3. Results

3.1. Inhibitory effect of MDL73811 derivatives on heterologous monofunctional PfAdoMetDC and bifunctional PfAdoMetDC/ODC

MDL73811 and Genz-644131 showed the highest percentage inhibition of monofunctional *Pf*AdoMetDC at 98% and 100%, respectively ($n = 3$, $P < 0.01$, paired Student's *t*-test) (Fig. 1). The inhibition of the *Pf*AdoMetDC domain of heterologous bifunctional *Pf*AdoMetDC/ODC was similar at 96% and 98%, respectively ($n = 3$, $P < 0.01$, paired Student's *t*-test) (Fig. 1). By contrast, Genz-644043 only inhibited monofunctional *Pf*AdoMetDC by 57% ($n = 3$, $P = 0.14$, paired Student's *t*-test) whereas Genz-644053 had no inhibitory effect (Fig. 1).

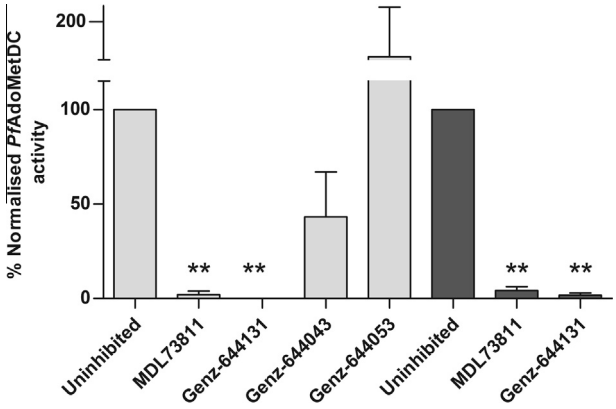

Fig. 1. The inhibitory activities of MDL73811 derivatives against monofunctional *Pf*AdoMetDC (grey) and the *Pf*AdoMetDC domain of bifunctional *Pf*AdoMetDC/ODC (black). MDL73811 and the three derivatives (1 μM) were incubated with either 5 μg monofunctional *Pf*AdoMetDC or bifunctional *Pf*AdoMetDC/ODC for 30 min at 37 °C. Specific activity (nmol/min/mg) of the monofunctional and bifunctional *Pf*AdoMetDC domains were normalised against the uninhibited enzymes. Data are representative of three independent experiments performed in triplicate, ±SEM. $^{**}P < 0.01$, paired Student's *t*-test. Where not shown, the error bars fall within the symbols.

The activity of *Pf*AdoMetDC decreased in a concentration dependent manner following pre-incubation with Genz-644131 for both monofunctional and bifunctional forms of the protein (Fig. 2A and C). A non-significant increase in the $K_i$app value of 0.36 ± 0.10 μM ($n = 3$, $P > 0.05$, unpaired Student's *t*-test) was determined for Genz-644131 on monofunctional *Pf*AdoMetDC (Fig. 2B) compared to 0.22 ± 0.09 μM for MDL73811 (results not shown). However, there was a significant difference in the inhibition of bifunctional *Pf*AdoMetDC/ODC by Genz-644131 ($K_i$app at 0.18 ± 0.02 μM (Fig. 2D) compared to MDL73811 (0.53 ± 0.09 μM, results not shown) ($n = 3$, $P = 0.02$, unpaired Student's *t*-test).

The efficiency of inactivation (depicted by the k_{inact}/K_iapp ratio) of MDL73811 compared to Genz-644131 against monofunctional *Pf*AdoMetDC was not significantly different at 1.91 and 1.17 μM^{-1} - min^{-1}, respectively. However, the inactivation efficiency for Genz-644131 against the *Pf*AdoMetDC domain of bifunctional *Pf*AdoMetDC/ODC is 1.6-fold higher (k_{inact}/K_iapp = 3.50 μM^{-1} min^{-1}) compared to MDL73811 (k_{inact}/K_iapp = 2.19 μM^{-1} min^{-1}). Moreover, there was a ~3-fold increase in the inactivation efficiency of Genz-644131 against bifunctional *Pf*AdoMetDC/ODC compared to monofunctional *Pf*AdoMetDC (k_{inact}/K_iapp ratios of 3.50 vs. 1.17 μM^{-1} min^{-1}), respectively. Genz-644131 seems to therefore be a more effective inhibitor of *Pf*AdoMetDC compared to MDL73811, with marked preference for the protein when found in its native conformation in bifunctional *Pf*AdoMetDC/ODC.

Due to the observed differences in the inhibition of MDL73811 and its derivatives against *Pf*AdoMetDC, the binding capacity of these compounds to *Pf*AdoMetDC was analysed *in silico*. Previously, it was shown that purine nucleoside AdoMetDC inhibitors adopt

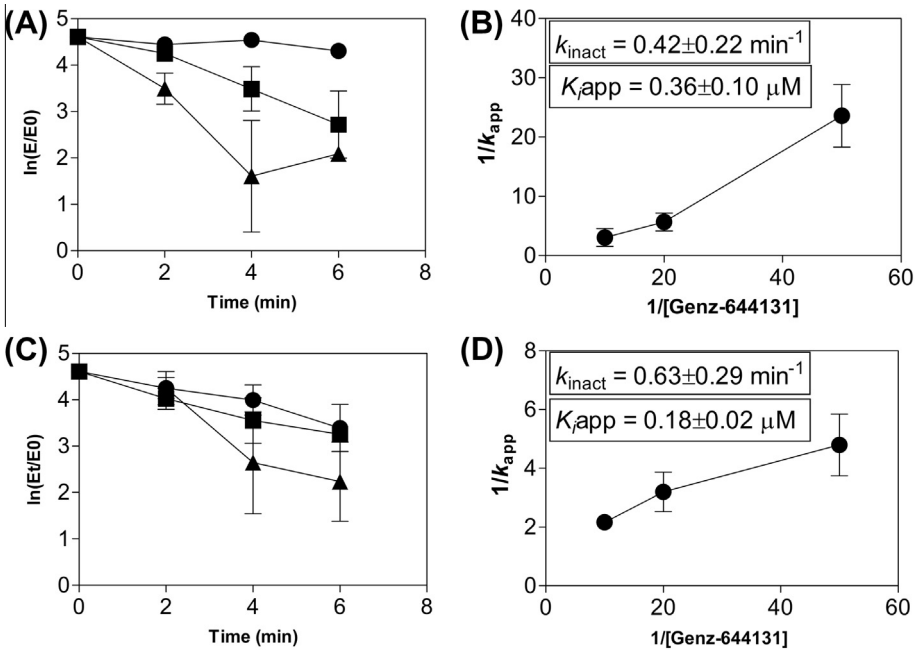

Fig. 2. Enzyme kinetics of Genz-644131 against monofunctional and bifunctional *Pf*AdoMetDC. Kitz-Wilson inhibition kinetics was used to determine the $K_i$app for Genz-644131 against monofunctional (A and B) and bifunctional *Pf*AdoMetDC (C and D). Percentage activity was determined from residual enzyme activity, following pre-incubation with Genz-644131 at 0.02 (circles), 0.05 (squares) or 0.1 μM (triangles) concentrations ([I]) at specific time intervals (0–6 min) (E_t). The $\ln(E_t/E_0)$ of the activity at a specific inhibitor concentration was plotted against the pre-incubation time points using non-linear regression. The reciprocal of the slopes ($1/k_{app}$) of the primary plots (A and C) was plotted against the reciprocal of the specific inhibitor concentrations using non-linear regression (B and D), from which the k_{inact} (inverse of the y-intercept) and the $K_i$app (slope multiplied by k_{inact}) were derived (Kitz and Wilson, 1962). Data are representative of three independent experiments performed in triplicate, ±SEM and all values fell into the 95% confidence interval of the mean. Where not shown, the error bars fall within the symbols.

unusual *syn* conformations and that modification of these inhibitors does not only affect protein ligand interactions but also alter conformational preferences (Tolbert et al., 2001) (Supplemental data S1). MDL73811 has an energy difference of 7.6 kcal/mol between the lowest energy conformation and its bioactive *syn* conformation (Table 1). However, the 8-methyl substitution on the purine rings of MDL73811, yielding Genz-644131, increases the conformational preference for the bioactive *syn* conformation of the latter (energy difference equal to 2.2 kcal/mol, Table 1). By contrast, the energy differences for both the halogen substituted Genz-644043 and Genz-644053 derivatives were higher, with the latter also showing a distorted *N*-(Z)-4-aminobutenyl-*N*-methyl tail conformation due to interference of the chlorine substitution at position 2 of the purine ring (Supplemental data S1).

The selected binding pose of Genz-644131 (Fig. 3A) shows similar interactions to other AdoMetDC substrate analogues (Fig. 3B) (McCloskey et al., 2009). Moreover, conformational search analysis of the *N*-(Z)-4-aminobutenyl-*N*-methyl tail of Genz-644131 showed that the lowest absolute energy of the Genz-644131 *syn* conformation is reached when the tail assumes the predicted binding conformation (-126.9 kcal/mol) (Fig. 3C). Notably, the 8-methyl substitution on the purine ring does not show any steric hindrance within the protein active site and therefore would not negatively affect ligand binding.

3.2. Genz-644131 is active against in vitro intraerythrocytic P. falciparum parasites

The IC_{50} of the MDL73811 derivatives was determined on intraerythrocytic *P. falciparum* parasites *in vitro* (96 h incubation at 37 °C). Treatment of intraerythrocytic *P. falciparum* parasites with Genz-644131 resulted in a significant, 2-fold decrease in the IC_{50} compared to MDL73811 (IC_{50} = 0.97 ± 0.06 μM vs. 2.21 ± 0.07 μM, $n = 5$, $P < 0.01$, unpaired Student's *t*-test). The IC_{50} values of Genz-644043 and Genz-644053 against intraerythrocytic *P. falciparum* parasites were significantly higher (25.6 ± 8.4 and 22.4 ± 7.5 μM; $n = 4$, $P > 0.05$, unpaired Student's *t*-test) than that of the parent compound, MDL73811.

The ability of exogenous polyamines to rescue the inhibitory effect of Genz-644131 on intraerythrocytic *P. falciparum* parasites was established by determining the IC_{50} of Genz-644131 in the presence and absence of exogenous spermidine (250 μM). No significant change in the IC_{50} value of Genz-644131 in the presence (IC_{50} = 0.94 ± 0.03 μM) or absence (IC_{50} = 0.97 ± 0.06 μM) of spermidine ($n = 3$, $P = 0.89$, paired Student's *t*-test) was observed (Fig. 4A), indicating that spermidine could not antagonise the inhibitory effect of Genz-644131. However, *P. falciparum* infected erythrocytes are capable of taking up exogenous spermidine, with [^{3}H]spermidine reaching a distribution ratio of 1.4 ± 0.4 ($n = 6$) following 60 min incubation (Fig. 4B).

The recovery of intraerythrocytic *P. falciparum* parasites (1% parasitaemia, 1% haematocrit) after limited exposure to Genz-644131 (2× IC_{50}) for 24 h was determined after washing out the compound, followed by additional incubation of parasite cultures for a further 96 h before measuring DNA content as an indicator of parasite proliferation. There was a significant increase in DNA levels observed for untreated parasites over the two life-cycles analysed (Fig. 4C). Genz-644131 treated ring-stage intraerythrocytic *P. falciparum* parasites (2× IC_{50}) were able to recover after 24 h of drug pressure and continue to proliferate following drug removal (Fig. 4C). However, continuous exposure of intraerythrocytic *P. falciparum* parasites to Genz-644131 (2× IC_{50}) for 96 h resulted in a stage-specific inhibition of parasite proliferation, with parasites arrested in the trophozoite stage (~24 h post-invasion) within the first life-cycle (Fig. 4D).

3.3. Effect of Genz-644131 encapsulated in nanovectors on in vitro antiplasmodial activity

To improve membrane translocation of Genz-644131 and possibly the *in vitro* activity against intraerythrocytic *P. falciparum* parasites, Genz-644131 was encapsulated into two types of nanovectors, a submicron micellular emulsion formulation, Pheroid® (Grobler et al., 2008), and a parasite targeting immunoliposome system (Urbán et al., 2011a). The compound encapsulated into Pheroid® did not show a significant decrease in the *in vitro* IC_{50} (0.97 ± 0.06 μM compared to 0.67 ± 0.29 μM; $n = 4$, $P > 0.05$,

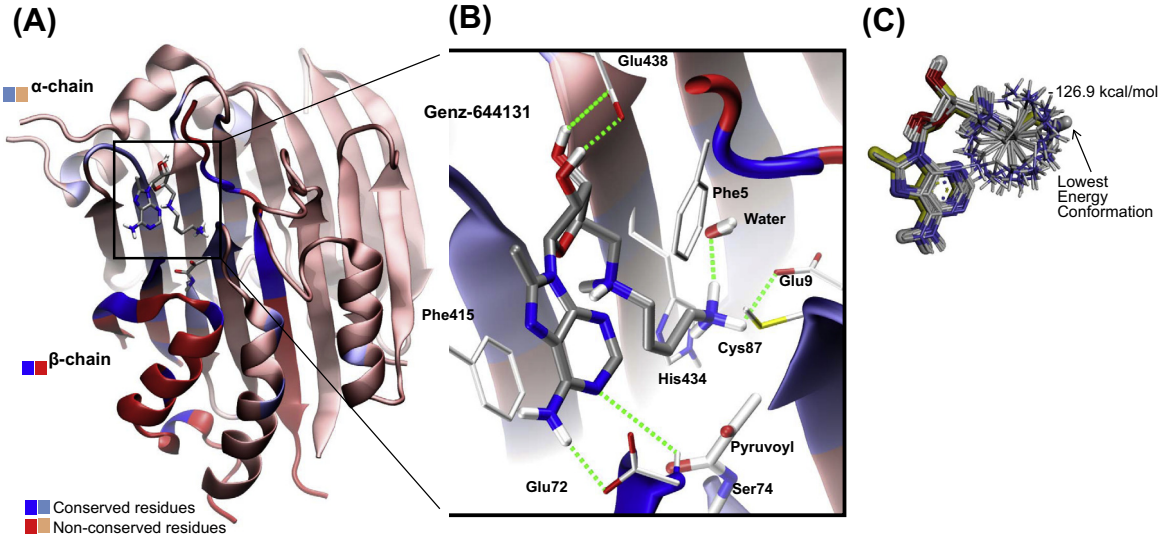

Fig. 3. A predicted binding pose for Genz-644131 to *Pf*AdoMetDC highlighting conserved residues with *T. brucei* and human protein equivalents. (A) A homology model of *Pf*AdoMetDC bound with Genz-644131 in the active site. The ribbon representing the β-chain is coloured either bright blue or red indicating conserved and non-conserved residues. Likewise, the α-chain ribbon is coloured in a lighter shade. (B) The interacting residues between *Pf*AdoMetDC and Genz-644131. Green lines represent hydrogen bonds formed between the protein and ligand. (C) Representation of the systematic conformational search of the [(Z)-4-amino-2-butenyl] methylamino tail with the lowest energy conformations in yellow. (For interpretation of the references to colour in this figure legend, the reader is referred to the web version of this article.)

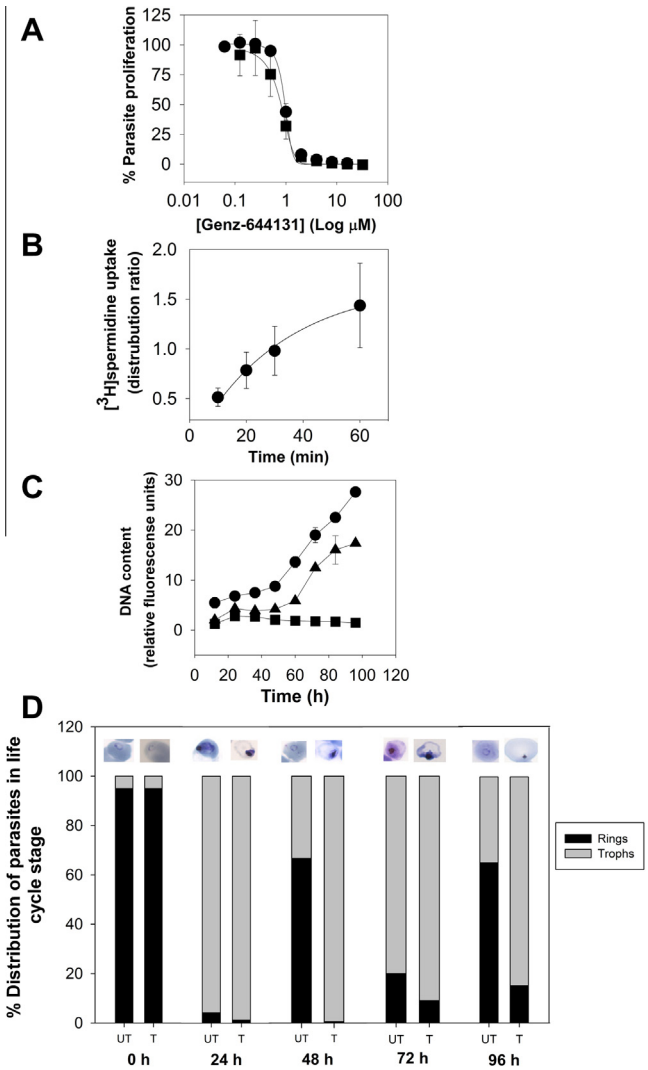

Fig. 4. Uptake of [^{3}H]spermidine, with rescue and reversibility of Genz-644131 inhibited intraerythrocytic *P. falciparum* parasites *in vitro*. (A) Initial ring stage intraerythrocytic *P. falciparum* parasites were treated with Genz-644131 (serial dilution) alone (squares) or in the presence of 250 μM spermidine (circles, 0.5 μM aminoguanidine present) for 96 h at 37 °C. Parasite proliferation is expressed as a percentage of untreated parasite proliferation at 100%. Data are representative of $n \geqslant 3$ independent experiments performed in triplicate, ± SEM. (B) Time course for the uptake of [^{3}H]spermidine (5 nM extracellular concentration) into intraerythrocytic *P. falciparum* parasites (circles) at 37 °C over 60 min averaged from five independent experiments and shown ± SEM. A distribution ratio of 1.4 ± 0.4 was obtained, where a ratio of 1 indicates that the radiolabelled polyamine has equilibrated to levels equal to the extracellular levels. (C) Initial ring stage intraerythrocytic *P. falciparum* parasites were either treated with Genz-644131 ($2 \times IC_{50}$, squares) for 96 h at 37 °C or treated with Genz-644131 ($2 \times IC_{50}$, triangles) for 24 h at 37 °C before replacing the culture media thereby removing the Genz-644131 before incubating the parasites for a further 96 h at 37 °C. Untreated initial ring stage intraerythrocytic *P. falciparum* parasites (circles) incubated at 37 °C for 96 h was included as a positive control for parasite proliferation. Samples were taken every 12 h and DNA content was measured as relative fluorescence units using SYBR Green I-based assay. Data are representative of $n \geqslant 3$ independent experiments performed in triplicate, ±SEM. Where not shown, the error bars fall within the symbol. (D) Morphological monitoring of the stage specificity of parasites treated with Genz-644131 ($2 \times IC_{50}$), analysing percentage distribution in each life-cycle stage. Treated parasites indicated that Genz-644131 arrested parasite development during the trophozoite stage compared to untreated parasites.

unpaired Student's *t*-test; Fig. 5A). By contrast, Genz-644131 encapsulated immunoliposomes showed a significant 32-fold decrease in the *in vitro* IC_{50} compared to non-encapsulated Genz-644131 (0.97 ± 0.06 μM vs. 0.031 ± 0.004 μM; $n = 3$, $P < 0.01$, unpaired Student's *t*-test) (Fig. 5B).

4. Discussion

Polyamine biosynthesis enzymes have been the target of various parasitic disease intervention strategies (Birkholtz et al., 2011) as highlighted by the clinical treatment of *T. brucei* infections through DFMO inhibition of ODC activity (Van Nieuwenhove et al., 1985). Of the other enzymatic activities associated with polyamine biosynthesis, inhibition of AdoMetDC shows promise as a therapeutic target in *P. falciparum*, with MDL73811 a 1000-fold more potent against intraerythrocytic *P. falciparum* parasites compared to DFMO (Wright et al., 1991). Although MDL73811 is an irreversible inhibitor of AdoMetDC activity, it has poor drug-like characteristics for *Plasmodium* (Wright et al., 1991) and *Trypanosoma* parasites (Barker et al., 2009), which led to the synthesis of pharmacokinetically amenable derivatives. These derivatives of MDL73811 were used here to determine (1) their efficacy in inhibiting the *Pf*AdoMetDC protein and (2) their antiproliferative activity against intraerythrocytic *P. falciparum* parasites *in vitro*.

Several comparisons can be drawn between the treatment of *P. falciparum* and *T. brucei* parasites with the lead derivative, Genz-644131. Firstly, the AdoMetDC protein from both these parasites responds similarly to Genz-644131 treatment. *Pf*AdoMetDC has a near conserved active site compared to AdoMetDC homologues from human and *T. brucei* parasites, despite an overall low sequence identity (21% and 23%, respectively (Wells et al., 2006)). As a result, MDL73811 inhibits AdoMetDC from both *P. falciparum* and *T. brucei* parasites at comparable levels and in a similar manner as indicated by their respective micromolar $K_i$app values (Bitonti et al., 1990; Das Gupta et al., 2005; Williams et al., 2011). However, Genz-644131 potently inhibits monofunctional and bifunctional *Pf*AdoMetDC similarly to *Tb*AdoMetDC (Barker et al., 2009) with $K_i$app values in the nanomolar range (Barker et al., 2009).

The 1.6-fold decrease in $K_i$app between MDL73811 and Genz-644131 observed for the bifunctional *Pf*AdoMetDC/ODC is explained by the 8-methyl substitution on the purine ring of Genz-644131, which promotes the preferred bioactive *syn* conformation (Pegg, 2009). However, Genz-644131 is ~7-fold less effective in inhibiting monofunctional *Pf*AdoMetDC compared to the *T. brucei* enzyme (k_{inact}/K_iapp ratios of 1.17 $\mu M^{-1}\,min^{-1}$ for *Pf*AdoMetDC compared to 7.78 $\mu M^{-1}\,min^{-1}$ for *Tb*AdoMetDC (Barker et al., 2009)). The association of *Pf*AdoMetDC with ODC in the biologically relevant bifunctional protein *Pf*AdoMetDC/ODC has been shown to result in the modulation of plasmodial AdoMetDC activity (Birkholtz et al., 2011; Williams et al., 2011). Rate-limiting and equimolar synthesis of putrescine and dcAdoMet by the ODC and AdoMetDC activities is enabled by a decrease in AdoMetDC activity when associated in the bifunctional complex with ODC in comparison to its monofunctional *Pf*AdoMetDC form, respectively (Williams et al., 2011). Here, although comparative inactivation efficiencies are seen for Genz-644131 for the monofunctional and bifunctional proteins, this inhibitor shows a ~3-fold increase in specificity and rate of inhibition of the AdoMetDC domain of the bifunctional protein. This can be attributed to the lower substrate K_m of *Pf*AdoMetDC in the bifunctional protein compared to the monofunctional protein, which probably reflects differences between active site conformations of these two proteins and consequently, their binding affinities for Genz-644131 (Williams et al., 2011). Interestingly, the simultaneous inhibition of both activities of the bifunctional *Pf*AdoMetDC/ODC with Genz-644131 and DFMO is additive as was also shown for MDL73811 and DFMO on *in vitro P. falciparum* parasites (Wright et al., 1991; van Brummelen et al., 2008) (Supplemental data S2).

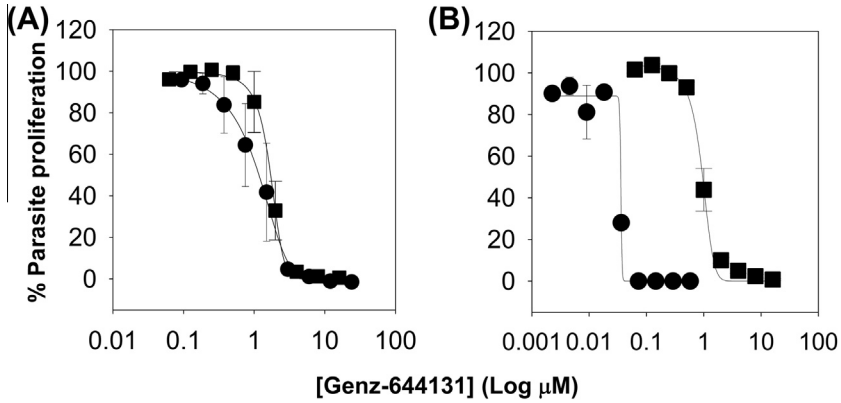

Fig. 5. The effect of encapsulation of Genz-644131 in different nanovectors on its *in vitro* anti-plasmodial activity. Parasite proliferation of ring stage intraerythrocytic *P. falciparum* parasites was monitored with a SYBR Green I-based assay over 96 h at 37 °C and IC_{50} determined from dilution series. Dose–response curves for Genz-644131 alone (squares) compared to incorporated into (A) Pheroid® or (B) immunoliposomes (circles). Data are representative in each instance of three independent experiments performed in triplicate or quadruplicate, ±SEM. Where not shown, the error bars fall within the symbols.

In contrast to the marked improvement (>10-fold) in the *in vitro* antiproliferative efficacy of *T. brucei* parasites treated with Genz-644131 compared to MDL73811 (Barker et al., 2009), Genz-644131 only shows marginal (2-fold) improvement in the *in vitro* IC_{50} against intraerythrocytic *P. falciparum* parasites. The antiproliferative effect observed with Genz-644131 was not plasmodicidal to the parasite, similar to treatment with MDL73811 and DFMO, with parasite proliferation recovering after limited Genz-644131 exposure (24 h at 2× IC_{50}). Both MDL73811 and DFMO treatment result in a cytostatic effect since inhibition is negated by the uptake of exogenous polyamines (Assaraf et al., 1987; Das Gupta et al., 2005). Co-treatment of parasites with MDL73811 and exogenous spermidine did not abolish the inhibitory effect of MDL73811 on parasite proliferation, and it was previously suggested that intraerythrocytic *P. falciparum* parasites are incapable of spermidine uptake, since exogenously supplied putrescine, but not spermidine, was capable of overcoming biosynthesis inhibition caused by a variety of inhibitors (Assaraf et al., 1987; Das Gupta et al., 2005). Likewise, co-treatment of parasites with Genz-644131 and exogenous spermidine also did not abolish the inhibitory effect of Genz-644131 on parasite proliferation. However, recent work clearly indicates that exogenous spermidine is taken up by isolated *P. falciparum* trophozoite-stage parasites (Niemand et al., 2012). Once inside the infected erythrocyte unit, the parasite is able to efficiently take up spermidine across the plasma membrane in a concentration dependent manner, mediated by an electrogenic process energised by the parasite's membrane potential (Niemand et al., 2012). In addition, here we report that exogenous spermidine is taken up by *P. falciparum* infected erythrocytes. Therefore, the inability of spermidine to abolish Genz-644131 inhibition does not appear to be due to the inability of the parasite to take up spermidine. Genz-644131 shows improved *in vivo* cellular toxicity against different *T. brucei* parasite strains (Bacchi et al., 2009; Barker et al., 2009). When this compound was tested in a murine malaria model for *in vivo* antimalarial activity, Genz-644131 significantly ($P < 0.001$) reduced *P. berghei* parasitaemia by 89% when dosed in the Peters model for 4 days at 100 mg/kg/day. Animals dosed with 20 mg/kg/day showed a 37% ($P = 0.002$) reduction. However, in no case was there sterile cure, as all animals had detectable parasitaemia levels on day 4 (Supplemental data S3). This may be due to the cytostatic effect described above.

The evidence provided does however not exclude the possibility of off target effects of Genz-644131 on *P. falciparum* parasites including its binding to purine deaminases and polyamine oxidases as observed for MDL73811 (Hirth et al., 2009), particularly to *P. falciparum* adenosine deaminases (Reyes et al., 1982) and erythrocytic polyamine oxidases (Byers et al., 1992). However, Genz-644131 (at 2× IC_{50}) arrested parasite development in a stage-specific manner during the trophozoite stages (18–26 h post invasion), as previously described for MDL73811 (Wright et al., 1991). This corresponds to the requirement of polyamines due to the stage-specific expression of *Pf*AdoMetDC/ODC (18–30 h post-invasion) during the trophozoite stage of the asexual cycle (van Brummelen et al., 2008). The parasite arrested temporal phenotype induced by Genz-644131 therefore corresponds to the expression profile of *Pf*AdoMetDC in the parasite as the target for this compound.

Another explanation for the relatively poor activity of Genz-644131 against intraerythrocytic *P. falciparum* parasites may be due to the poor membrane permeability of the compound itself, as low membrane permeability was previously shown to be the only inferior *in vitro* ADME characteristic of the MDL73811 derivatives (Barker et al., 2009). Additionally, for any compound to access the intraerythrocytic *P. falciparum* parasites, they would need to cross the parasite plasma membrane (PPM), parasitophorous vacuolar membrane (PVM) and erythrocyte membrane (Lingelbach and Joiner, 1998). Extracellular *T. brucei* parasites are surrounded by only a single plasma membrane (Vennerstrom et al., 2004; Orhan et al., 2006) and cannot synthesise purines *de novo*, and therefore have to acquire host purines (Hassan and Coombs, 1988). Adenosine, of which MDL73811 is a structural analogue, is actively transported into *T. brucei* parasites by the *T. brucei* nucleotide transporter 1 (*Tb*NT1) (de Koning et al., 2005) and the *T. brucei* aminopurine transporter (*Tb*AT1 or P_2). The latter transporter has been confirmed to actively transport MDL73811 (Goldberg et al., 1997; Maser et al., 1999), which could explain the low nanomolar *in vitro* IC_{50} values of MDL73811 in these parasites. As in *T. brucei*, *Plasmodium* parasites also do not synthesise purines *de novo* and has to recruit exogenous purines from the host (Downie et al., 2008). In contrast to *T. brucei*, multiple transport mechanisms enable the uptake of purines into intraerythrocytic *P. falciparum* parasites including host purine transporters (Quashie et al., 2008) as well as parasite derived transporters, *Pf*NT1 and *Pf*NT4 localised in the PPM (Carter et al., 2000; Parker et al., 2000). Although the latter are low-affinity transporters (Downie et al., 2008), their ability to transport MDL73811 and derivatives needs further investigation.

The development of novel lipid based nanovectors provides a solution for the challenges facing malaria chemotherapeutics, since it has the potential to mediate sustained, targeted drug release thereby increasing the drug plasma half-life, lowering dosage requirements and reducing drug toxicity (Maurer et al., 2011). Additionally, lipid-based nanovectors has been shown to eliminate off-target effects by delivery to specific targeted cells, thereby improving the therapeutic efficacy of the compound (Forrest and Kwon, 2008). This makes lipid based nanovector drug delivery systems ideal for treatment of intracellular pathogens (Alving, 1986; Armstead and Bingyun, 2011; Maurer et al., 2011). Previous encapsulations of chloroquine (Urbán et al., 2011a) and fosmidomycin (Urbán et al., 2011b) resulted in a 10- and 7.5-fold decrease in the *in vitro* IC_{50} values of these compounds.

To investigate possible enhancement of the uptake of Genz-644131 into intraerythrocytic *P. falciparum* parasites, the compound was incorporated into two nanovector drug delivery systems: Pheroid® and immunoliposomes (Steyn et al., 2011; Urbán et al., 2011a). The Pheroid® system is a nanovector carrier developed from a submicron micellular emulsion formulation, typically ranging in size from 80 to 300 nm (Steyn et al., 2011). These micellular structures can be manipulated in terms of structure, size and morphology to enhance the solubility properties of intended compounds, by entrapment and delivery of compounds across cellular membranes (Steyn et al., 2011). Liposomes are synthetic lipid bilayers of up to 200 nm that have the ability to increase drug bioavailability by encapsulating compounds into the hydrophilic core of the lipid bilayer system. Moreover, the liposomal preparations were orientated with half anti-glycophorin A antibodies, specific for intraerythrocytic *P. falciparum* parasites, enhancing the selectivity of Genz-644131 to the parasite (Urbán et al., 2011a). Here, the 32-fold decrease observed in the *in vitro* IC_{50} of immunoliposome encapsulated Genz-644131 against intraerythrocytic *P. falciparum* parasites suggests that the uptake of Genz-644131 by itself into intracellular *P. falciparum* parasites is restricted. However, the activity of compounds can be improved by either enhancing the chemical pharmacokinetic properties through medicinal chemistry, or encapsulating the compound into drug delivery systems. Although the Genz-644131 immunoliposome combination has not been tested *in vivo*, other immunoliposomal drug suspensions tested against murine mice infections improved the pharmacokinetic profiles of the drugs tested (Owais et al., 1995; Agrawal and Gupta, 2000). Encapsulation of Genz-644131 with immunoliposomes may also reduce non-specific off-target effects and in an sustainable release of the drug to prolong its plasma half-life.

The combination of Genz-644131 with a novel nanovector drug delivery system therefore provides the most promising result obtained thus far with this nanovector delivery system against intraerythrocytic *P. falciparum* parasites *in vitro*, and could be evaluated in novel antimalarial drug development.

Acknowledgements

We would like to thank Liezl-Marie Scholtz at the DST/NWU Preclinical Drug Development Platform. This work was supported by the Department of Science and Technology through the South African Malaria Initiative, the University of Pretoria, the South African National Research Foundation and by grant BIO2011-25039 from the Ministerio de Economía y Competitividad, Spain, which included FEDER funds, and 2009SGR-760 from the Generalitat de Catalunya, Spain. All studies were conducted under protocols approved by the IACUC of the Medical Sciences campus, University of Puerto Rico and in accordance with the Guide for the Care and Use of Laboratory Animals (National-Research-Council. 1996. Guide for the Care and Use of Laboratory Animals. National Academy Press, Washington, DC).

Appendix A. Supplementary data

Supplementary data associated with this article can be found, in the online version, at http://dx.doi.org/10.1016/j.ijpddr.2013.11.003.

References

Agrawal, A.K., Gupta, C.M., 2000. Tuftsin-bearing liposomes in treatment of macrophage-based infections. Adv. Drug Deliv. Rev. 41, 135–146.
Alving, C.R., 1986. Liposomes as drug carriers in leishmaniasis and malaria. Parasitol. Today 2, 101–107.
Armstead, A.L., Bingyun, L., 2011. Nanomedicine as an emerging approach against intracellular pathogens. Int. J. Nanomed. 6, 3281–3293.
Assaraf, Y.G., Golenser, J., Spira, D.T., Messer, G., Bachrach, U., 1987. Cytostatic effect of DL-α-difluoromethylornithine against *Plasmodium falciparum* and its reversal by diamines and spermidine. Parasitol. Res 73, 313–318.
Bacchi, C.J., Barker, R.H., Rodriguez, A., Hirth, B., Rattendi, D., Yarlett, N., Hendrick, C.L., Sybertz, E., 2009. Trypanocidal activity of 8-methyl-5′-{[(Z)-4-aminobut-2-enyl]-(methylamino)} adenosine (Genz 644131), an adenosylmethionine decarboxylase inhibitor. Antimicrob. Agents Chemother. 53, 3269–3271.
Barker, R.H., Hanlan, L., Hirth, B., Celatka, C.A., Fitzpatrick, R., Xiang, Y., Willert, E.K., Phillips, M.A., Kaiser, M., Bacchi, C.Y., 2009. Novel S-adenosylmethionine decarboxylase inhibitors for the treatment of human African trypanosomiasis. Antimicrob. Agents Chemother. 53, 2052–2058.
Birkholtz, L., Wrenger, C., Joubert, F., Wells, G.A., Walter, R.D., Louw, A.I., 2004. Parasite-specific inserts in the bifunctional *S*-adenosylmethionine decarboxylase/ornithine decarboxylase of *Plasmodium falciparum* modulate catalytic activities and domain interactions. Biochem. J. 15, 439–448.
Birkholtz, L., Williams, M., Niemand, J., Louw, A.I., Persson, L., Heby, O., 2011. Polyamine homoeostasis as a drug target in pathogenis protozoa: peculiarities and possibilities. Biochem. J. 438, 229–244.
Bitonti, A.J., Byers, T.L., Bush, T.L., Casara, P.J., Bacchi, C.J., Clarkson Jr., A.B., McCann, P.P., Sjoerdsma, A., 1990. Cure of *Trypanosoma brucei brucei* and *Trypanosoma brucei rhodesiense* infections in moe with an irreversible inhibitor of S-adenosylmethionine decarboxylase. Antimicrob. Agents Chemother. 34, 1485–1490.
Byers, T.L., Bush, T.L., McCann, P.P., Bitonti, A.J., 1991. Antitrypanosomal effects of polyamine biosynthesis inhibitors correlate with increases in *Trypanosoma brucei brucei* S-adenosyl-L-methionine. Biochem. J. 274, 527–533.
Byers, T.L., Ganem, B., Pegg, A.E., 1992. Cytostasis induced in L1210 murine leukaemia cells by the S-adenosyl-L-methionine decarboxylase inhibitor 5′-([(Z)-4-amino-2-butenyl]methylamino)-5′-deoxyadenosine may be due to hypusine depletion. Biochem. J. 287, 717–724.
Carter, N.S., Mamoun, C.B., Liu, W., Silva, E.O., Landfear, S.M., Goldberg, D.E., Ullman, B., 2000. Isolation and functional characterization of the *Pf*NT1 nucleoside transporter from *Plasmodium falciparum*. J. Biol. Chem. 275, 28153–28157.
Casero, R.A., Marton, L.J., 2007. Targeting polyamine metabolism and function in cancer and other hyperproliferative diseases. Nat. Rev. Drug Discov. 6, 373–390.
Das Gupta, R., Krause-Ihle, T., Bergmann, B., Müller, I.B., Khomut, A.R., Müller, S., Walter, R.D., Lüersen, K., 2005. 1-Aminooxy-3-aminopropane and derivatives have an antiproliferative effect on cultured *Plasmodium falciparum* by decreasing intracellular polyamine concentrations. Antimicrob. Agents Chemother. 49, 2857–2864.
de Koning, H.P., Bridges, D.J., Burchmore, R.J., 2005. Purine and pyrimidine transport in pathogenic protozoa: from biology to therapy. FEMS Microbiol. Rev. 29, 987–1020.
Downie, M.J., Kirk, K., Mamoun, C.B., 2008. Purine salvage pathways in the intraerythrocytic malaria parasite *Plasmodium falciparum*. Eukaryot. Cell 7, 1231–1237.
Forrest, M.L., Kwon, G.S., 2008. Clinical developments in drug delivery nanotechnology. Adv. Drug Deliv. Rev. 60, 861–862.
Goldberg, B., Yarlett, N., Sufrin, J., LLoyd, D., Bacchi, C.Y., 1997. A unique transporter of *S*-adenosylmethionine in African trypanosomes. FASEB J. 11, 256–260.
Grobler, A., Kotzé, A., and Du Plessis, J., 2007. The design of a skin-friendly carrier for cosmetic compounds using Pheroid™ Technology. Delivery system technologies.
Grobler, A., Kotzé, A., and Du Plessis, J., 2008. The design of a skin-friendly carrier for cosmetic compounds using Pheroid™ Technology. Science and Applications of Skin Delivery System Technologies Allured. Ed. Johann Wiechers, 283–311.
Grobusch, M.P., Hanscheid, T., Gobels, K., Slevogt, H., Zoller, T., Rogler, G., Teichmann, D., 1998. Comparison of three antigen detection tests for diagnosis and follow-up of *falciparum* malaria in travellers returning to Berlin, Germany. Parasitol. Res. 89, 354–357.
Hassan, H.F., Coombs, G.H., 1988. Purine and pyrimidine metabolism in parasitic protozoa. FEMS Microbiol. Rev. 54, 47–84.
Heby, O., Roberts, S.C., Ullman, B., 2003. Polyamine biosynthetic enzymes as drug targets in parasitic protozoa. Biochem. Soc. Trans. 31, 415–419.
Heby, O., Persson, L., Rentala, M., 2007. Targeting the polyamine biosynthetic enzymes: a promising approach to therapy of African sleeping sickness, Chagas' disease and leishmaniasis. Amino Acids 33, 359–366.
Hirth, B., Barker, R.H., Celatka, C.A., Klinger, J.D., Liu, H., Nare, B., Nijjar, A., Phillips, M.A., Sybertz, E., Willert, E.K., et al., 2009. Discovery of new S-

adenosylmethionine decarboxylase inhibitors for the treatment of human African trypanosomiasis (HAT). Bioorg. Med. Chem. Lett. 19, 2916–2919.
Kitz, R., Wilson, I.B., 1962. Esters of methanesulfonic acid as irreversible inhibitors of acetylcholinesterase. J. Biol. Chem. 237, 3245–3249.
Lee, Y., Sayre, L.M., 1998. Reaffirmation that metabolism of polyamines by bovine plasma amine oxidase occurs strictly at the primary amino termini. J. Biol. Chem. 273, 19490–19494.
Lingelbach, K., Joiner, K.A., 1998. The parasitophorous vacuole membrane surrounding *Plasmodium* and Toxoplasma: an unusual compartment in infected cells. J. Cell Sci. 111, 1467–1475.
MacDonald, R.C., MacDonald, R.I., Menco, B.P., Takeshita, K., Subbarao, N.K., Hu, L.R., 1991. Small-volume extrusion apparatus for preparation of large, unilamellar vesicles. Biochim. Biophys. Acta 1061, 297–303.
Maser, P., Sutterlin, C.K., Kraminsky, R., 1999. A nucleoside transporter from *Trypanosoma brucei* involved in drug resistance. Science 285, 242–244.
Maurer, N., Fenske, D.B., Cullis, P.R., 2011. Developments in liposomal drug delivery systems. Expert Opin. Biol. Ther. 1, 923–947.
McCloskey, D.E., Bale, S., Secrist, J.A., Tiwari, A., Moss, T.H., Valiyaveettil, J., Brooks, W.H., Guida, W.C., Pegg, A.E., Ealick, S.E., 2009. New insights into the design of inhibitors of human S-adenosylmethionine decarboxylase: studies of adenine C(8) substitution in structural analogues of S-adenosylmethionine. J. Med. Chem. 52, 1388–1407.
Niemand, J., Louw, A.I., Kirk, K., Birkholtz, L., 2012. Polyamine uptake by the intraerythrocytic malaria parasite, *Plasmodium falciparum*. Int. J. Parasitol. 42, 921–929.
Niemand, J., Burger, P., Verlinden, B.K., Reader, J., Joubert, A.M., Kaiser, A., Louw, A.I., Kirk, K., Phantsiel, O., Birkholtz, L., 2013. Anthracene-polyamine conjugates inhibit in vitro proliferation of intraerythrocytic *Plasmodium falciparum* parasites. Antimicrob. Agents Chemother. 57, 2874–2877.
Orhan, I., Sener, B., Atici, T., Brun, R., Perozzo, R., Tasdemir, D., 2006. Turkish freshwater and marine macrophyte extracts show *in vitro* antiprotozoal actvity and inhibit FabI, a key enzyme of *Plasmodium falciparum* fatty acid biosynthesis. Phytomedicine 13, 388–393.
Owais, M., Varshney, G.C., Choudhury, A., Chandra, S., Gupta, C.M., 1995. Chloroquine encapsulated in malaria-infected erythrocyte-specific antibody-bearing liposomes effectively controls chloroquine-resistant *Plasmodium berghei* infections in mice. Antimicrob. Agents Chemother. 39, 180–184.
Parker, M.D., Hyde, R.J., Yao, S.Y.M., McRobert, L., Cass, C., Young, J.D., McConkey, G.A., Baldwin, S.A., 2000. Identification of a nucleoside/nucleobase transporter from *Plasmodium falciparum*, a novel target for anti-malarial chemotherapy. Biochem. J. 349, 67–75.
Pegg, A.E., 2006. Regulation of ornithine decarboxylase. J. Biol. Chem. 281, 14529–14532.
Pegg, A.E., 2009. S-adenosylmethionine decarboxylase. Essays Biochem. 46, 25–45.
Quashie, N.B., Ranford-Cartwright, L.C., de Koning, H.P., 2008. A comprehensive model of purine uptake by the malaria parasite *Plasmodium falciparum*: identification of four purine transport activities in intraerythrocytic parasites. Biochem. J. 411, 287–295.
Reyes, P., Rathod, P.K., Sanchez, D.J., Mrema, J.E., Rieckamn, K.H., Heidrich, H.G., 1982. Enzymes of purine and pyrimidine metabolism from the human malaria parasite, *Plasmodium falciparum*. Mol. Biochem. Parasitol. 5, 275–290.
Saliba, K.J., Horner, H.A., Kirk, K., 1998. Transport and metabolism of the essential vitamin pantothenic acid in human erythrocytes infected with the malaria parasite *Plasmodium falciparum*. J. Biol. Chem. 273, 10190–10195.
Steyn, J.D., Wiesner, L., du Plessis, L.H., Grobler, A.F., Smith, P.J., Chan, W.-C., Haynes, R.K., Kotzé, A.F., 2011. Absorption of the novel artemisinin derivatives artemisone and artemiside: potential application of Pheroid™ Technology. Int. J. Pharm. 414, 260–266.
Stjernborg, L., Persson, L., 1993. Stabilization of S-adenosylmethionine decarboxylase by aminoguanidine. Biochem. Pharmacol. 45, 1174–1176.
Teng, R.W., Junankar, P.R., Bubb, W.A., Rae, C., Mercier, P., Kirk, K., 2009. Metabolite profiling of the intraerythrocytic malaria parasite *Plasmodium falciparum* by H-1 NMR spectroscopy. NMR Biomed. 22, 292–302.
Tolbert, W.D., Ekstrom, J.L., Mathews, I.I., Secrist, J.A., Kapoor, P., Pegg, A.E., Ealick, S.E., 2001. The structural basis for substrate specificity and inhibition of human S-adenosylmethionine decarboxylase. Biochemistry 40, 9484–9494.
Trang, D.T.X., Huy, N.T., Kariu, T., Tajima, K., Kamei, K., 2004. One-step concentration of malarial parasite-infected red blood cells and removal of contaminating white blood cells. Malar. J. 3, http://dx.doi.org/10.1186/1475-2875-3-7.
Urbán, P., Estelrich, J., Cortes, A., Fernandez-Busquets, X., 2011a. A nanovector with complete discrimination for targeted delivery to *Plasmodium falciparum*-infected versus non-infected red blood cells *in vitro*. J. Control Release 151, 202–211.
Urbán, P., Estelrich, J., Adeva, A., Cortés, A., Fernàndez-Busquets, X., 2011b. Study of the efficacy of antimalarial drugs delivered inside targeted immunoliposomal nanovectors. Nanoscale Res. Lett. 6, 1–9.
van Brummelen, A.C., Olszewski, K.L., Wilinski, D., Llinas, M.L., Louw, A.I., Birkholtz, L., 2008. Co-inhibition of *Plasmodium falciparum S*-adenosylmethionine decarboxylase/ornithine decarboxylase reveals perturbation-specific compensatory mechanisms by transcriptome, proteome and metabolome analysis. J. Biol. Chem. 284, 4635–4646.
Van Nieuwenhove, S., Schechter, P.J., Declercq, J., Bone, G., Burke, J., Sjoerdsma, A., 1985. Treatment of gambiense sleeping sickness in the Sudan with oral DFMO (DL-α-difluoromethylornithine), an inhibitor of ornithine decarboxylase: first field trial. Trans. R. Soc. Trop. Med. Hyg. 79, 692–698.
Vennerstrom, J.L., Arbe-Barnes, S., Brun, R., Charman, S.A., Chiu, F.C.K., Chollet, J., Dong, Y., Dorn, A., Hunziker, D., Matile, H., et al., 2004. Identification of an antimalarial synthetic trioxolane drug development candidate. Nature 430, 900–904.
Verlinden, B.K., Niemand, J., Snyman, J., Sharma, S.K., Beattie, R.J., Woster, P.M., Birkholtz, L., 2011. Discovery of novel alkylated (bis)urea and (bis)thiourea polyamine analogues with potent antimalarial activities. J. Med. Chem. 54, 6624–6633.
Wallace, H.M., Fraser, A.V., Hughes, A., 2003. A perspective of polyamine metabolism. Biochem. J. 376, 1–14.
Wells, G., Birkholtz, L., Joubert, F., Walter, R., Louw, A.I., 2006. Novel properties of malarial S-adenosylmethionine decarboxylase as revealed by structural modelling. J. Mol. Graph Mod. 24, 307–318.
Willert, E.K., Phillips, M.A., 2008. Regulated expression of an essential allosteric activator of polyamine biosynthesis in African trypanosomes. PLoS Pathog. 4, http://dx.doi.org/10.1371/journal.ppat.1000183.
Williams, M., Sprenger, J., Human, E., Al-Karadaghi, S., Persson, L., Louw, A.I., Birkholtz, L., 2011. Biochemical characterization and novel classification of monofunctional *S*-adenosylmethionine decarboxylase of *Plasmodium falciparum*. Mol. Biol. Parasitol. 180, 17–26.
Wright, P.S., Byers, T.L., Cross-Doersen, D.E., McCann, P.P., Bitonti, A.J., 1991. Irreversible inhibition of S-adenosylmethionine decarboxylase in *Plasmodium falciparum*-infected erythrocytes: growth inhibition *in vitro*. Biochem. Pharmacol. 41, 1713–1718.
Yarlett, N., Quamina, A., Bacchi, C., 1991. Protein methylases in *Trypanosoma brucei brucei:* activities and response to DL-α-difluoromethylornithine. J. Microbiol. 137, 717–724.